

## Band-structure reorganization across the magnetic transition in BaFe<sub>2</sub>As<sub>2</sub> seen via high-resolution angle-resolved photoemission

Guodong Liu,<sup>1</sup> Haiyun Liu,<sup>1</sup> Lin Zhao,<sup>1</sup> Wentao Zhang,<sup>1</sup> Xiaowen Jia,<sup>1</sup> Jianqiao Meng,<sup>1</sup> Xiaoli Dong,<sup>1</sup> Jun Zhang,<sup>1</sup> G. F. Chen,<sup>1</sup> Guilong Wang,<sup>2</sup> Yong Zhou,<sup>2</sup> Yong Zhu,<sup>2</sup> Xiaoyang Wang,<sup>2</sup> Zuyan Xu,<sup>2</sup> Chuangtian Chen,<sup>2</sup> and X. J. Zhou<sup>1,\*</sup>

<sup>1</sup>Beijing National Laboratory for Condensed Matter Physics, Institute of Physics, Chinese Academy of Sciences, Beijing 100190, China

<sup>2</sup>Technical Institute of Physics and Chemistry, Chinese Academy of Sciences, Beijing 100190, China  
(Received 25 March 2009; revised manuscript received 23 August 2009; published 23 October 2009)

High-resolution angle-resolved photoemission measurements have been carried out on BaFe<sub>2</sub>As<sub>2</sub>, a parent compound of the FeAs-based superconductors. In the magnetic ordering state, there is no gap opening observed on the Fermi surface. Instead, dramatic band-structure reorganization occurs across the magnetic transition. The appearance of the singular Fermi spots near  $(\pi, \pi)$  is the most prominent signature of magnetic ordering. These observations provide direct evidence that the magnetic ordering state of BaFe<sub>2</sub>As<sub>2</sub> is distinct from the conventional spin-density-wave state. They reflect the electronic complexity in this multiple-orbital system and necessity in involving the local magnetic moment in describing the underlying electron structure.

DOI: 10.1103/PhysRevB.80.134519

PACS number(s): 74.25.Jb, 74.70.-b, 79.60.-i, 71.20.-b

The interplay between magnetism and superconductivity is a prominent topic in the recently discovered FeAs-based superconductors.<sup>1-3</sup> The ground state of the parent compound of the FeAs-based superconductors has a collinear antiferromagnetic ordering.<sup>4-6</sup> Superconductivity is achieved from suppressing the magnetic ordering by chemical doping<sup>1-3</sup> or application of high pressure.<sup>7</sup> Magnetism has been proposed to play an important role in generating high-temperature superconductivity in this new class of high-temperature superconductors.<sup>8,9</sup> However, the nature of the magnetic ordering and its origin remain under hot debate.<sup>4,10</sup> It is proposed that the magnetic ordering is associated with the spin-density-wave (SDW) formation driven by the Fermi-surface nesting.<sup>4</sup> Recent optical<sup>11</sup> and quantum oscillation<sup>12</sup> measurements reported gap opening related with the magnetic transition which is in favor of the SDW picture. It becomes critical to pin down whether there is really a gap opening and, if there is, where the gap opens in the momentum space. In principle, angle-resolved photoemission (ARPES) measurements can provide direct information on these issues but so far the ARPES results remain inconclusive.<sup>13-21</sup>

In this paper we report angle-resolved photoemission evidence to show the unusual nature of magnetic ordering in a parent compound of FeAs-based superconductors, BaFe<sub>2</sub>As<sub>2</sub>.<sup>22</sup> Unlike the conventional SDW system<sup>23</sup> where magnetic ordering is associated with Fermi-surface nesting and a gap opening,<sup>24</sup> the electronic structure of BaFe<sub>2</sub>As<sub>2</sub> shows no sign of gap opening on the Fermi surface in the magnetically ordered state. Instead, it shows a dramatic band reorganization and particularly an emergence of singular strong Fermi spots. These observations provide direct and clear-cut evidences that the magnetic ordering state of BaFe<sub>2</sub>As<sub>2</sub> is distinct from the conventional SDW state. They also point to the importance and necessity in involving the local magnetic moment in the underlying electron structure. These results and their understanding will have important implications on understanding the magnetism and superconductivity in this new class of superconductors.

The ARPES measurements are carried out on our photoemission system equipped with Scienta R4000 electron-energy analyzer and helium-discharge lamp which gives a photon energy of  $h\nu=21.218$  eV.<sup>25</sup> The light on the sample is partially polarized. The energy resolution was set at 10 meV and the angular resolution is  $\sim 0.3^\circ$ . The Fermi level is referenced by measuring on the Fermi edge of a clean polycrystalline gold that is electrically connected to the sample. The BaFe<sub>2</sub>As<sub>2</sub> single crystals were grown using flux method<sup>11</sup> which show a magnetic/structural transition at  $T_{MS} \sim 138$  K.<sup>11,22</sup> The crystals were cleaved *in situ* and measured in vacuum with a base pressure better than  $5 \times 10^{-11}$  Torr. For ARPES measurements, we found that the cleaved surface of BaFe<sub>2</sub>As<sub>2</sub> shows a change with time. To reduce the influence of this aging effect, we took many independent measurements on fresh surfaces. All the Fermi-surface-mapping measurements reported here were taken within four hours after cleaving (Fig. 1), and for the typical momentum cuts (Fig. 2), the measurements were carried out within two hours after cleaving.

In the magnetic ordering state, the Fermi surface of BaFe<sub>2</sub>As<sub>2</sub> near the  $\Gamma$  point shows three hole-like sheets [Fig. 1(a)], as evidenced from Figs. 2(a) and 2(d) where three Fermi crossings are clearly resolved in the bands taken along the  $\Gamma$ -M1( $\pi, \pi$ ) direction [Cut 1 in Fig. 1(a)]. For the convenience of description, we denote the four M points as M1( $\pi, \pi$ ), M2( $-\pi, \pi$ ), M3( $-\pi, -\pi$ ), and M4( $\pi, -\pi$ ). The corresponding Fermi momenta are  $\sim 0.06$ ,  $\sim 0.20$ , and  $\sim 0.35\pi/a$ , respectively. Additional measurements along  $\Gamma$ -X( $\pi, 0$ ) and other directions also give three Fermi crossings with similar Fermi momenta.

The most prominent features in the Fermi-surface topology of BaFe<sub>2</sub>As<sub>2</sub> below  $T_{MS}$  are the strong Fermi spots near M points [Fig. 1(a)], labeled as S1 and S2 near the M2( $-\pi, \pi$ ) point, and S3 and S4 near the M3( $-\pi, -\pi$ ) point. In these two independent measurements near M2 and M3 [Fig. 1(a)] under different geometries, the strong spots are only obvious along the  $\Gamma$ -M direction, with a distance between them (S1 and S2, or S3 and S4) at  $\sim 0.65\pi/a$ . To

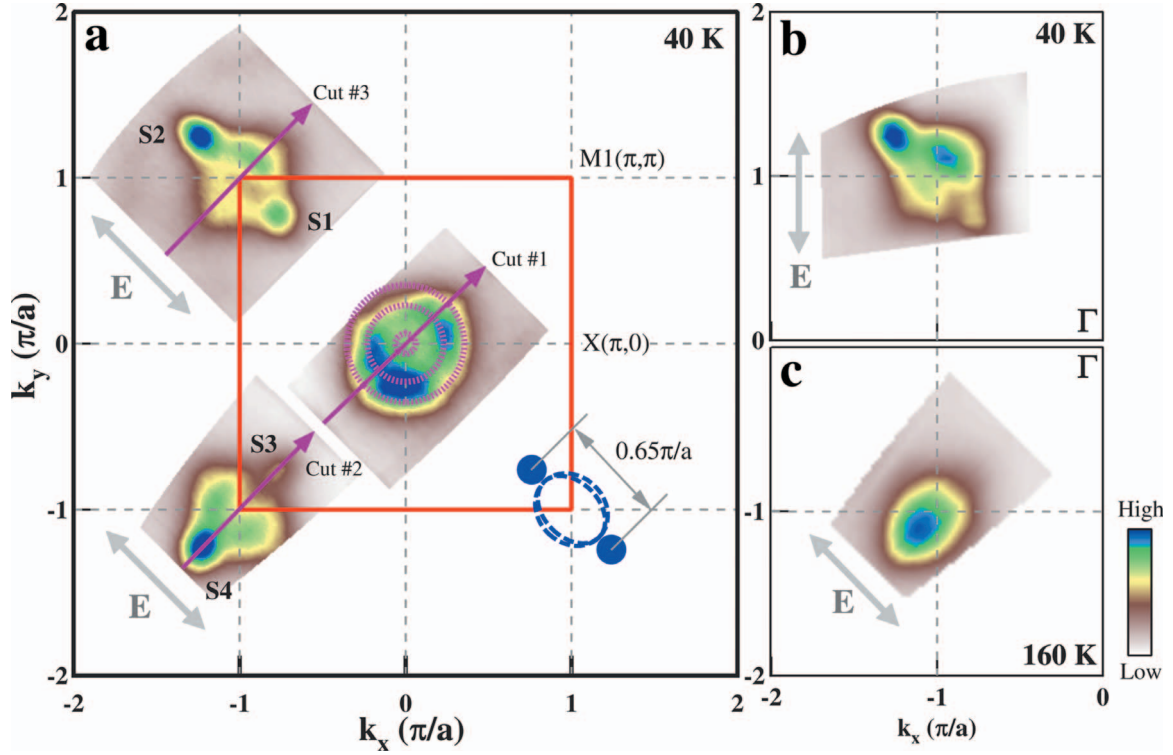


FIG. 1. (Color) Fermi surface of BaFe<sub>2</sub>As<sub>2</sub> above and below the magnetic transition temperature ( $T_{MS}=138$  K). (a) Spectral-weight distribution integrated within  $(-10$  and  $10$  meV) energy window with respect to the Fermi level as a function of  $k_x$  and  $k_y$  measured at 40 K. All the data were taken with the major electric vector along the  $(\pi, -\pi) - (-\pi, \pi)$  diagonal direction, as shown by the double-headed arrows. (b) Fermi surface near the M2 point measured at 40 K with the main electric vector along  $(0, 0) - (0, \pi)$  vertical direction. (c) Fermi surface near M3  $(-\pi, -\pi)$  measured at 160 K.

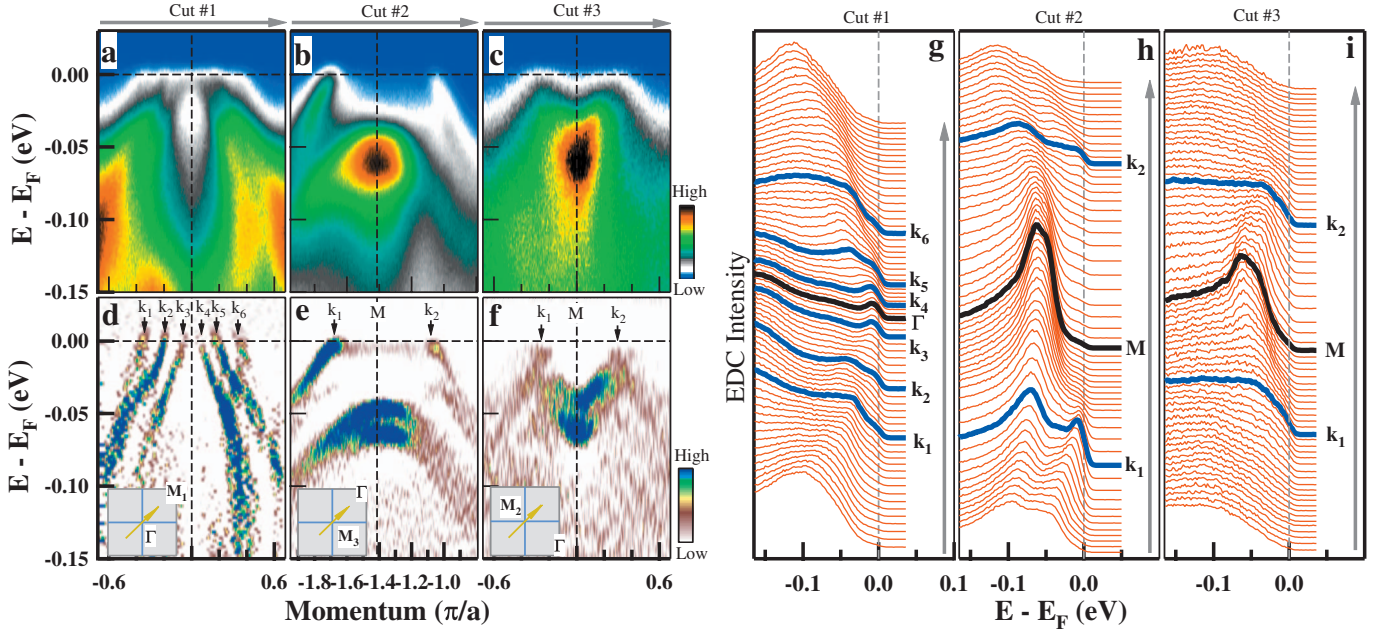


FIG. 2. (Color) Band structure and photoemission spectra of BaFe<sub>2</sub>As<sub>2</sub> along typical high-symmetry cuts measured at 20 K. [(a), (b), and (c)] show original photoemission images measured along the three high-symmetry cuts (Cuts 1, 2, and 3 in Fig. 1(a)). The location of the three cuts are also shown in the insets of (d), (e), and (f). To highlight underlying band structure more clearly, (d), (e), and (f) show corresponding second derivative images. (g), (h), and (i) show photoemission spectra EDCs for the three cuts with those near the Fermi momenta and high-symmetry points colored and marked.

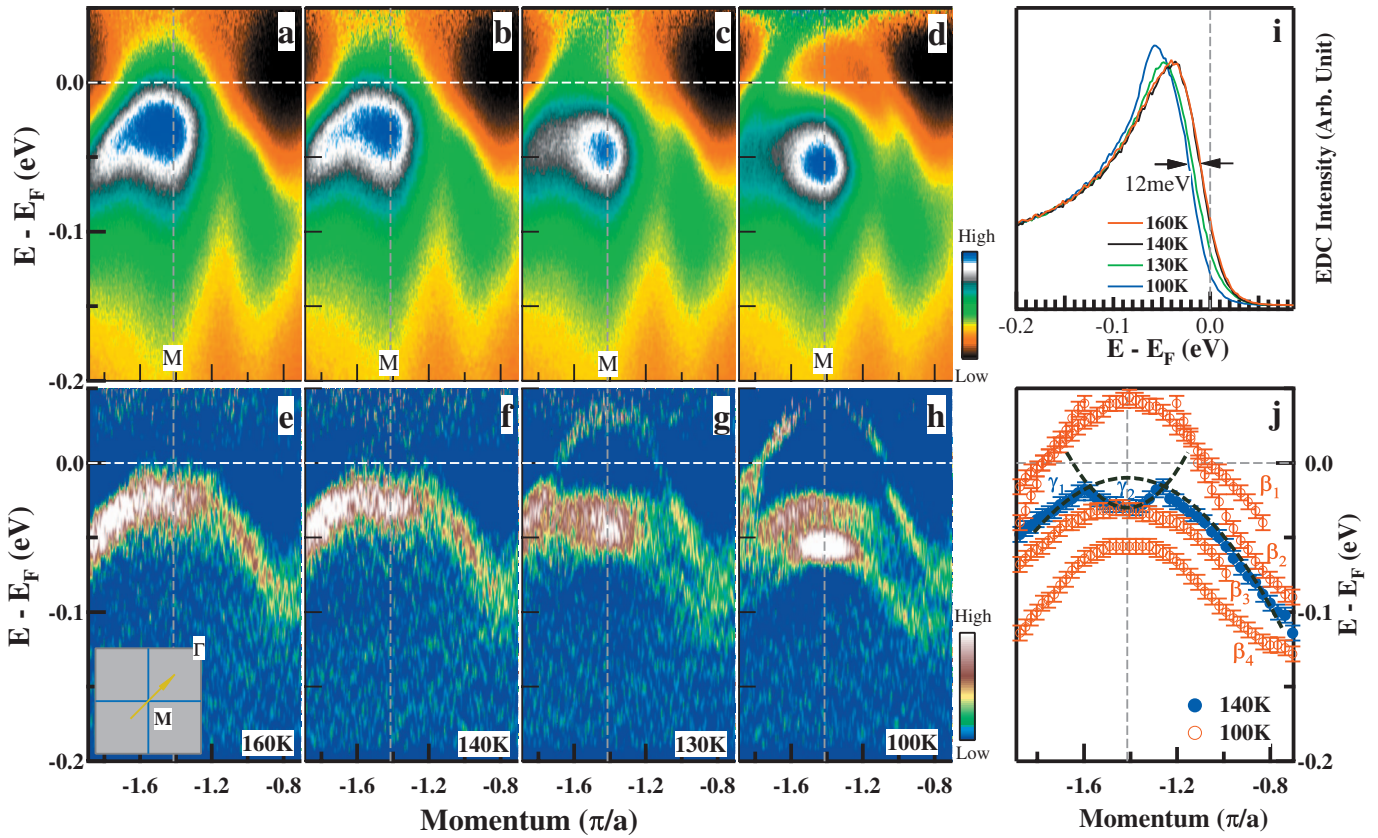


FIG. 3. (Color) Dramatic band reorganization of  $\text{BaFe}_2\text{As}_2$  across the magnetic transition near the  $M(\pi, \pi)$  point. [(a)–(d)] Photoemission images taken along the  $(0, 0) - (\pi, \pi)$  direction near the  $M3(-\pi, -\pi)$  point at different temperatures. The location of the cut is similar to the Cut 2 in Fig. 1(a) and also shown in the inset of (e). These images are obtained from the original data divided by the Fermi-distribution function which allows to observe the electronic states above the Fermi level. [(e)–(h)] The corresponding second derivative images. (i) Photoemission spectra (EDCs) at the  $M$  point measured at different temperatures. (j) Measured bands at 140 (blue solid circles) and 100 K (red empty circles). The data involve symmetrization with respect to the  $M$  point. The black dashed lines are guide to the eyes showing the band above  $T_{MS}$  appears to be composed of two bands: one hole like ( $\gamma_1$ ) and one electron like ( $\gamma_2$ ).

check whether this could be affected by the matrix-element effect associated with the particular electric vector, we took another measurement with a different polarization geometry and observed similar pattern [Fig. 1(b)], suggesting a weak polarization dependence. These strong spots disappear above the magnetic transition temperature,  $T_{MS}$ , [Fig. 1(c)], and therefore are intimately related with the magnetic ordering state.

In addition to the strong spots, there are also intensity patches on both sides of the  $\Gamma - M2(M3)$  line(s) [Fig. 1(a)]. Band-structure measurements [Figs. 2(c) and 2(f) for the Cut 3 in Fig. 1(a)] indicate they originate from the electron-like bands. The Fermi-surface topology near the  $M$  point below  $T_{MS}$  is therefore composed of two electron-like Fermi-surface sheets and two strong Fermi spots, as schematically shown in the bottom-right quadrant of Fig. 1(a). Note that the strong Fermi spots are not part of the electron-like Fermi-surface sheets because they originate from different bands (Fig. 2).

It is well known that the conventional SDW formation such as in Cr (Ref. 23) is associated with a gap opening along the nested section of Fermi surface.<sup>24</sup> It remains under debate whether similar mechanism operates in the magnetic ordering state in the parent compound of FeAs-based

superconductors.<sup>4,10</sup> The detailed Fermi-surface and band-structure results allow us to directly examine on this issue. Considering the nesting vector in  $\text{BaFe}_2\text{As}_2$  close to  $(0, 0) - (\pi, \pi)$ ,<sup>4</sup> the most likely locations to search for possible gap opening are close to the Fermi-surface sections near the  $\Gamma - M$  line [Cut 2 and its equivalent cuts in Fig. 1(a)]. It is clear from Fig. 2(g) that, near the  $\Gamma$  point, all photoemission spectra at the Fermi momenta cross the Fermi level, showing no gap opening along  $\Gamma - M$  direction. Measurements along other sections of three Fermi-surface sheets near  $\Gamma$  see no signature of gap opening either. Furthermore, there is no gap opening seen for the strong Fermi spots [Fig. 2(h)] and for the two electron-like Fermi-surface sheets [Fig. 2(i)]. These results provide a direct evidence that the magnetic ordering state of  $\text{BaFe}_2\text{As}_2$  does not involve gap opening which is fundamentally different from the conventional SDW system.<sup>23,24</sup>

The band structure of  $\text{BaFe}_2\text{As}_2$  experiences a dramatic reorganization across  $T_{MS}=138$  K near the  $M$  point, in terms of both the number of bands and their energy position (Fig. 3). Above  $T_{MS}$ , only one major branch of band is resolved [Figs. 3(a), 3(b), 3(e), and 3(f)]. As plotted in a more quantitative manner in Fig. 3(j), it appears to be composed of a hole-like band ( $\gamma_1$ ) and an electron-like band ( $\gamma_2$ ). Below

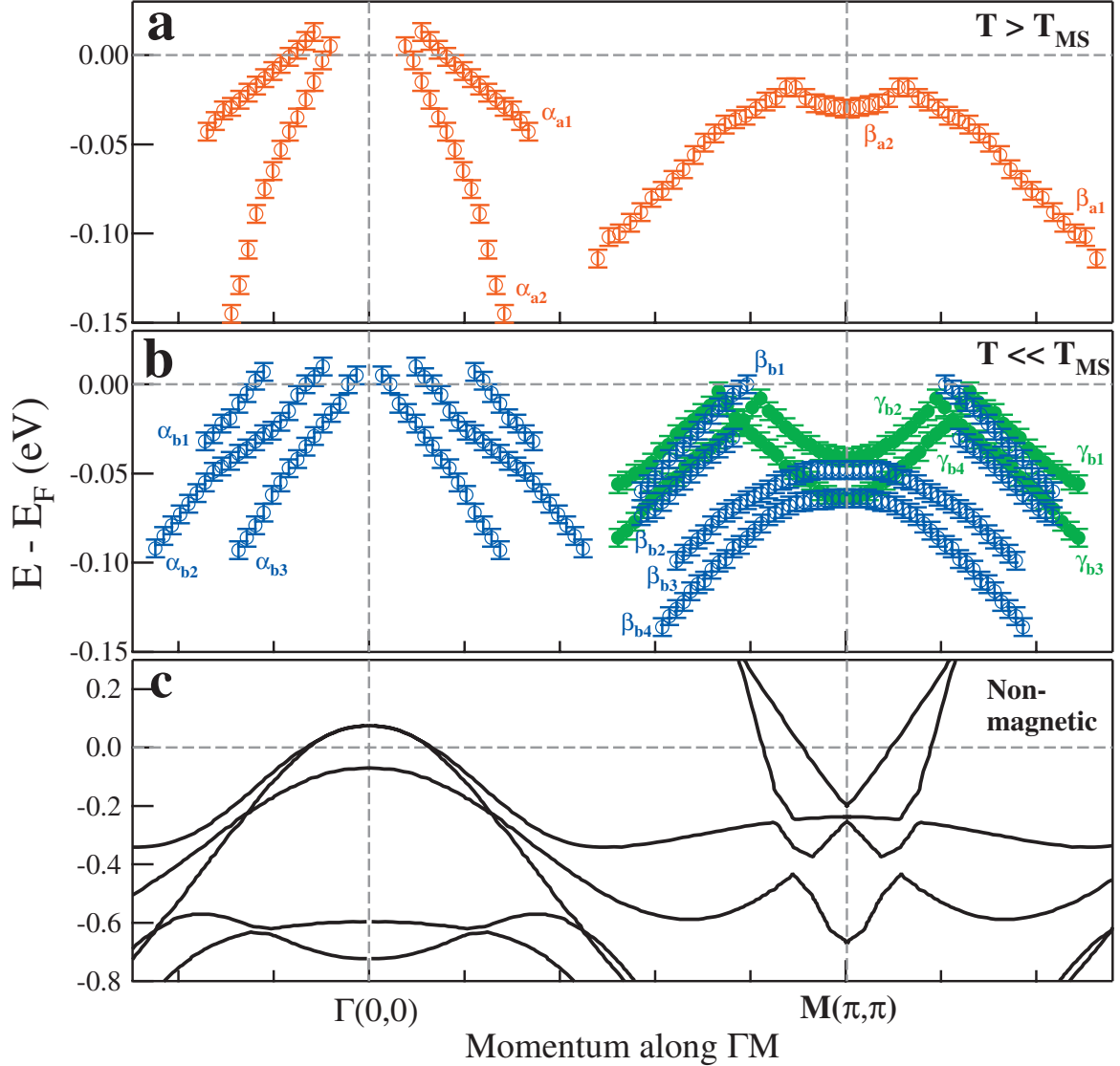


FIG. 4. (Color) Band structure of  $\text{BaFe}_2\text{As}_2$  along the  $\Gamma$ - $M$  high-symmetry line above (a) and below (b)  $T_{MS}$ . Below  $T_{MS}$  (b), the bands near the  $M$  point are from two measurements: Cut 2 in Fig. 2(b) (blue empty circles) and Cut 3 in Fig. 2(c) (green solid circles). (c) Electronic structure of  $\text{BaFe}_2\text{As}_2$  from band calculations in a nonmagnetic state (Refs. 31–33).

$T_{MS}$ , four bands emerge with inverse-parabolic shape [Figs. 3(c), 3(d), 3(g), 3(h), and 3(j)]: two of them [ $\beta_1$  and  $\beta_2$  in Fig. 3(j)] crossing the Fermi level while the other two below the Fermi level [ $\beta_3$  and  $\beta_4$  in Fig. 3(j)]. Such a band-structure change is remarkable considering its occurrence within a narrow temperature window between 140 K [Figs. 3(b) and 3(f)] and 130 K [Figs. 3(c) and 3(g)]. This also indicates that ARPES signal is sensitive to the magnetic transition at a temperature that is consistent with the bulk  $\text{BaFe}_2\text{As}_2$  material. The obvious band evolution with temperature can also be seen from the photoemission spectra at the  $M$  point [Fig. 3(i)]. Above  $T_{MS}=138$  K, the energy distribution curves (EDCs) at  $M$  point are similar at 140 and 160 K. Upon entering the magnetic ordering state, the EDC first shifts downward with a leading-edge movement of  $\sim 12$  meV at 130 K. Further decreasing of temperature gives rise to the splitting of the original one EDC peak into two features: one peak and one shoulder with a  $\sim 20$  meV apart,

which correspond to the two inverse-parabolic bands near  $M$  [ $\beta_3$  and  $\beta_4$  in Fig. 3(j)].

The striking difference of the band structure of  $\text{BaFe}_2\text{As}_2$  above  $T_{MS}$  [Fig. 4(a)] and below  $T_{MS}$  [Fig. 4(b)] clearly indicates that the magnetic ordering state does not inherit its electronic structure simply from its high-temperature nonmagnetic counterpart. It was reported that there is a three-dimension (3D) to two-dimension (2D) crossover associated with the magnetic/structural transition.<sup>26,27</sup> But because the Fermi surfaces near the  $M$  region remain quasi 2D and unaffected by such a transition,<sup>26</sup> 3D to 2D transition cannot explain the dramatic band-structure reorganization and change in the Fermi surface we have observed near the  $M$  point. A natural question is whether such a strong band reorganization can be attributed to the band-folding effect associated with the magnetic/structural transition. Such a transition renders the initial  $\Gamma$  and  $M$  points equivalent in the new shrunk Brillouin zone causing the bands at  $\Gamma$  and  $M$  to fold

to each other. In principle, such a band-folding effect is always present regardless of the origin of the magnetic ordering. In real experiment, whether the folded bands can be resolved depends on the interaction potential and matrix-element effect: the intensity of the folded bands can be much weaker than the primary ones.<sup>28,29</sup> Such a folding effect was previously proposed to account for the magnetic transition in  $\text{SrFe}_2\text{As}_2$ .<sup>20</sup> But our observations indicate it is not the main contributor to the dramatic band reorganization (Fig. 4). The two hole-like bands below the Fermi level near M [ $\beta_{b3}$  and  $\beta_{b4}$  in Fig. 4(b)] definitely cannot be due to the band-folding effect because there are no corresponding bands near  $\Gamma$ . For the same reason, the innermost band near  $\Gamma$  [ $\alpha_{b3}$  in Fig. 4(b)] cannot be due to such a band folding from M either. As for the two hole-like bands crossing the Fermi level near M [ $\beta_{b1}$  and  $\beta_{b2}$  in Fig. 4(b)], they appear similar to the bands near  $\Gamma$  and one may wonder whether they may originate from the folding effect. However, from the bands in Fig. 3(j) where the bands near and above  $E_F$  are clearly visible (Fig. 3), the two hole-like bands cross each other near  $E_F$ . This observation makes them unlikely to originate from the two bands near  $\Gamma$  which are separate. The band folding is also expected to produce similar Fermi-surface topology near  $\Gamma$  and M. While the strong Fermi spots are obvious near M, no such replica can be identified near  $\Gamma$  point [Fig. 1(a)]. This further indicates that the folding effect in  $\text{BaFe}_2\text{As}_2$  is weak although, in principle, it is present.

The strong Fermi spots are most prominent electronic signature of magnetic ordering in  $\text{BaFe}_2\text{As}_2$  as they only appear below  $T_{MS}$  [Figs. 1(a) and 1(c)]. One natural way to form such a singular Fermi spots is to have two bands crossing near the Fermi level giving rise to a Dirac cone-like structure. In FeAs-based compounds with multiple bands, below  $T_{MS}$ , the folding between the hole-like bands near  $\Gamma$  and the electron-like bands near M can give rise to such Dirac nodes along  $\Gamma$ -M direction which are gapless.<sup>30</sup> These characteristics seem to be in qualitative agreement with our observations and similar folding picture was also used for a previous ARPES experiment.<sup>20</sup> However, some of our experimental observations are at variance with this picture. In the folding picture, the Dirac nodes are produced from one hole-like band folded from  $\Gamma$  to M and one electron-like band near M.<sup>20,30</sup> However, our results indicate that the spectral weight of the strong spots are mainly from the hole-like bands [Figs. 2(b) and 2(e)]. Figure 3(j) further suggests that the strong spots are more likely formed by the two hole-like bands ( $\beta_1$  and  $\beta_2$ ) crossing each other near the Fermi level. The contribution to the strong spots formation from the electron-like bands is weak because no trace of electron-like bands is resolved along the  $\Gamma$ -M direction [Figs. 2(b), 2(e), and 3] probably due to matrix-element effect.

We note that the strong Fermi spots we have observed [Fig. 1(a)] show some resemblance to the “propeller-shaped” pattern reported before for a given polarization in both  $\text{BaFe}_2\text{As}_2$  and  $(\text{Ba}_{1-x}\text{K}_x)\text{Fe}_2\text{As}_2$  superconductor which was attributed to “hidden”  $(\pi, \pi)$  excitations that exist all the way to room temperature.<sup>18</sup> Our results clearly indicate that the strong Fermi spots cannot originate from the same hidden  $(\pi, \pi)$  order because they appear only below  $T_{MS}$  (Figs. 1 and 3). We also observed strong Fermi spots near M in  $(\text{Ba}_{0.6}\text{K}_{0.4})\text{Fe}_2\text{As}_2$  superconductor.<sup>16</sup> In terms of the Fermi-surface topology, our observation of strong Fermi spots in both magnetically ordered  $\text{BaFe}_2\text{As}_2$  and superconducting  $(\text{Ba}_{0.6}\text{K}_{0.4})\text{Fe}_2\text{As}_2$  seems to be consistent with the previous experiment showing similar patterns.<sup>18</sup> However, the underlying band structure we have revealed between them is remarkably different.<sup>16</sup> This indicates that the seemingly similar strong Fermi spots in the parent (Fig. 1) and K doped  $\text{BaFe}_2\text{As}_2$  (Ref. 16) are most likely from different origins rather than from the same  $(\pi, \pi)$  excitations proposed before.<sup>18</sup>

The dramatic band reorganization across  $T_{MS}$  and the lack of gap opening provide clear-cut evidences that the magnetic ordering state of  $\text{BaFe}_2\text{As}_2$  is distinct from the usual SDW state.<sup>23,24</sup> These observations may provide an alternative approach to understand previous measurements.<sup>11,12</sup> For example, the multiple bands developed below  $T_{MS}$  [Fig. 4(b)] may provide additional channels for interband transitions, offering an alternative interpretation of gap opening in terms of SDW picture that was proposed in the optical spectroscopy.<sup>11</sup> Our results show that the multiple-band structure [Fig. 4(b)] and the appearance of strong Fermi spots [Fig. 1(a)] below  $T_{MS}$  are neither inherited from its high-temperature nonmagnetic state nor from the band-folding effect associated with the magnetic/structural transition. These indicate that they are electronic fingerprints inherent to the magnetic ordered state. These characteristics reflect the electronic complexity in this multiple-orbital system and point to the importance and necessity in involving the local magnetic moment in the underlying electron structure. How to describe the peculiar electronic features of the magnetically ordered state on a quantitative level presents a challenge to further theoretical work. Our observations and their understanding will shed light on understanding the magnetism and high-temperature superconductivity in FeAs-based superconductors.

We thank A. V. Balatsky, J. P. Hu, D. H. Lee, Z. Y. Lu, J. L. Luo, E. W. Plummer, N. L. Wang, and T. Xiang for helpful discussions. This work is supported by the NSFC, the MOST of China (973 Projects No. 2006CB601002 and No. 2006CB921302).

\*Corresponding author; xjzhou@aphy.iphy.ac.cn

- <sup>1</sup>Y. Kamihara, T. Watanabe, M. Hirano, and H. Hosono, *J. Am. Chem. Soc.* **130**, 3296 (2008).
- <sup>2</sup>Z. A. Ren, W. Lu, J. Yang, W. Yi, X. L. Shen, Z. C. Li, G. C. Che, X. L. Dong, L. L. Sun, F. Zhou, and Z. X. Zhao, *Chin. Phys. Lett.* **25**, 2215 (2008).
- <sup>3</sup>M. Rotter, M. Tegel, and D. Johrendt, *Phys. Rev. Lett.* **101**, 107006 (2008).
- <sup>4</sup>J. Dong, H. J. Zhang, G. Xu, Z. Li, G. Li, W. Z. Hu, D. Wu, G. F. Chen, X. Dai, J. L. Luo, Z. Fang, and N. L. Wang, *EPL* **83**, 27006 (2008).
- <sup>5</sup>C. de la Cruz, Q. Huang, J. W. Lynn, W. Jiyang Li, I. I. Ratcliff, J. L. Zarestky, H. A. Mook, G. F. Chen, J. L. Luo, N. L. Wang, and Pengcheng Dai, *Nature (London)* **453**, 899 (2008).
- <sup>6</sup>Q. Huang, Y. Qiu, Wei Bao, M. A. Green, J. W. Lynn, Y. C. Gasparovic, T. Wu, G. Wu, and X. H. Chen, *Phys. Rev. Lett.* **101**, 257003 (2008).
- <sup>7</sup>M. S. Torikachvili, S. L. Bud'ko, N. Ni, and P. C. Canfield, *Phys. Rev. Lett.* **101**, 057006 (2008); T. Park, E. Park, H. Lee, T. Klimczuk, E. D. Bauer, F. Ronning, and J. D. Thompson, *J. Phys.: Condens. Matter* **20**, 322204 (2008); P. L. Alireza, Y. T. Chris Ko, J. Gillett, C. M. Petrone, J. M. Cole, S. E. Sebastian, and G. G. Lonzarich, *ibid.* **21**, 012208 (2009).
- <sup>8</sup>I. I. Mazin, D. J. Singh, M. D. Johannes, and M. H. Du, *Phys. Rev. Lett.* **101**, 057003 (2008); K. Kuroki, S. Onari, R. Arita, H. Usui, Y. Tanaka, H. Kontani, and H. Aoki, *ibid.* **101**, 087004 (2008); F. Wang, H. Zhai, Y. Ran, A. Vishwanath, and D.-H. Lee, *ibid.* **102**, 047005 (2009); A. V. Chubukov, D. V. Efremov, and I. Eremin, *Phys. Rev. B* **78**, 134512 (2008); V. Stanev, J. Kang, and Z. Tesanovic, *ibid.* **78**, 184509 (2008); F. Wang, H. Zhai, and D.-H. Lee, *EPL* **85**, 37005 (2009); I. I. Mazin and M. D. Johannes, *Nat. Phys.* **5**, 141 (2009).
- <sup>9</sup>X. Dai, Z. Fang, Y. Zhou, and F.-C. Zhang, *Phys. Rev. Lett.* **101**, 057008 (2008); P. A. Lee and X. G. Wen, *Phys. Rev. B* **78**, 144517 (2008).
- <sup>10</sup>T. Yildirim, *Phys. Rev. Lett.* **101**, 057010 (2008); Q. M. Si and E. Abrahams, *ibid.* **101**, 076401 (2008); J. S. Wu, P. Phillips, and A. H. Castro Neto, *ibid.* **101**, 126401 (2008); C. Fang, H. Yao, W.-F. Tsai, J. P. Hu, and S. A. Kivelson, *Phys. Rev. B* **77**, 224509 (2008); C. Xu, M. Muller, and S. Sachdev, *ibid.* **78**, 020501(R) (2008); S. P. Kou, T. Li, and Z. Weng, arXiv:0811.4111 (unpublished).
- <sup>11</sup>W. Z. Hu, J. Dong, G. Li, Z. Li, P. Zheng, G. F. Chen, J. L. Luo, and N. L. Wang, *Phys. Rev. Lett.* **101**, 257005 (2008).
- <sup>12</sup>S. E. Sebastian, J. Gillett, N. Harrison, P. H. C. Lau, C. H. Mielke, and G. G. Lonzarich, *J. Phys.: Condens. Matter* **20**, 422203 (2008).
- <sup>13</sup>L. X. Yang, Y. Zhang, H. W. Ou, J. F. Zhao, D. W. Shen, B. Zhou, J. Wei, F. Chen, M. Xu, C. He, Y. Chen, Z. D. Wang, X. F. Wang, T. Wu, G. Wu, X. H. Chen, M. Arita, K. Shimada, M. Taniguchi, Z. Y. Lu, T. Xiang, and D. L. Feng, *Phys. Rev. Lett.* **102**, 107002 (2009).
- <sup>14</sup>C. Liu, G. D. Samolyuk, Y. Lee, N. Ni, T. Kondo, A. F. Santander-Syro, S. L. Bud'ko, J. L. McChesney, E. Rotenberg, T. Valla, A. V. Fedorov, P. C. Canfield, B. N. Harmon, and A. Kaminski, *Phys. Rev. Lett.* **101**, 177005 (2008).
- <sup>15</sup>H. Y. Liu, W. T. Zhang, L. Zhao, X. W. Jia, J. Q. Meng, G. D. Liu, X. L. Dong, G. F. Chen, J. L. Luo, N. L. Wang, W. Lu, G. L. Wang, Y. Zhou, Y. Zhu, X. Y. Wang, Z. Y. Xu, C. T. Chen, and X. J. Zhou, *Phys. Rev. B* **78**, 184514 (2008).
- <sup>16</sup>L. Zhao, H. Y. Liu, W. T. Zhang, J. Q. Meng, X. W. Jia, G. D. Liu, X. L. Dong, G. F. Chen, J. L. Luo, N. L. Wang, G. L. Wang, Y. Zhou, Y. Zhu, X. Y. Wang, Z. X. Zhao, Z. Y. Xu, C. T. Chen, and X. J. Zhou, *Chin. Phys. Lett.* **25**, 4402 (2008).
- <sup>17</sup>H. Ding, P. Richard, K. Nakayama, T. Sugawara, T. Arakane, Y. Sekiba, A. Takayama, S. Souma, T. Sato, T. Takahashi, Z. Wang, X. Dai, Z. Fang, G. F. Chen, J. L. Luo, and N. L. Wang, *EPL* **83**, 47001 (2008).
- <sup>18</sup>V. B. Zabolotnyy, D. S. Inosov, D. V. Evtushinsky, A. Koitzsch, A. A. Kordyuk, G. L. Sun, J. T. Park, D. Haug, V. Hinkov, A. V. Boris, C. T. Lin, M. Knupfer, A. N. Yaresko, B. Buechner, A. Varykhalov, R. Follath, and S. V. Borisenko, *Nature (London)* **457**, 569 (2009).
- <sup>19</sup>Y. Zhang, J. Wei, H. W. Ou, J. F. Zhao, B. Zhou, F. Chen, M. Xu, C. He, G. Wu, H. Chen, M. Arita, K. Shimada, H. Namatame, M. Taniguchi, X. H. Chen, and D. L. Feng, *Phys. Rev. Lett.* **102**, 127003 (2009).
- <sup>20</sup>D. Hsieh, Y. Xia, L. Wray, D. Qian, K. Gomes, A. Yazdani, G. F. Chen, J. L. Luo, N. L. Wang, and M. Z. Hasan, arXiv:0812.2289 (unpublished).
- <sup>21</sup>M. Yi, D. H. Lu, J. G. Analytis, J.-H. Chu, S.-K. Mo, R.-H. He, R. G. Moore, X. J. Zhou, G. F. Chen, J. L. Luo, N. L. Wang, Z. Hussain, D. J. Singh, I. R. Fisher, and Z.-X. Shen, *Phys. Rev. B* **80**, 024515 (2009).
- <sup>22</sup>M. Rotter, M. Tegel, D. Johrendt, I. Schellenberg, W. Hermes and R. Pottgen, *Phys. Rev. B* **78**, 020503(R)(2008).
- <sup>23</sup>E. Fawcett, *Rev. Mod. Phys.* **60**, 209 (1988).
- <sup>24</sup>J. Schäfer, E. Rotenberg, G. Meigs, S. D. Kevan, P. Blaha, and S. Hufner, *Phys. Rev. Lett.* **83**, 2069 (1999).
- <sup>25</sup>G. D. Liu, G. L. Wang, Y. Zhu, H. B. Zhang, G. C. Zhang, X. Y. Wang, Y. Zhou, W. T. Zhang, H. Y. Liu, L. Zhao, J. Q. Meng, X. L. Dong, C. T. Chen, Z. Y. Xu, and X. J. Zhou, *Rev. Sci. Instrum.* **79**, 023105 (2008).
- <sup>26</sup>C. Liu, T. Kondo, N. Ni, A. D. Palczewski, A. Bostwick, G. D. Samolyuk, R. Khasanov, M. Shi, E. Rotenberg, S. L. Bud'ko, P. C. Canfield, and A. Kaminski, *Phys. Rev. Lett.* **102**, 167004 (2009).
- <sup>27</sup>P. Vilmercati, A. Fedorov, I. Vobornik, U. Manju, G. Panaccione, A. Goldoni, A. S. Sefat, M. A. McGuire, B. C. Sales, R. Jin, D. Mandrus, D. J. Singh, N. Mannella, *Phys. Rev. B* **79**, 220503(R) (2009).
- <sup>28</sup>J. Voit, L. Perfetti, F. Zwick, H. Berger, G. Margaritondo, G. Gruener, H. Hoehst, and M. Grioni, *Science* **290**, 501 (2000).
- <sup>29</sup>V. Brouet, W. L. Yang, X. J. Zhou, Z. Hussain, R. G. Moore, R. He, D. H. Lu, Z. X. Shen, J. Laverock, S. B. Dugdale, N. Ru, and I. R. Fisher, *Phys. Rev. B* **77**, 235104 (2008).
- <sup>30</sup>Y. Ran, F. Wang, H. Zhai, A. Vishwanath, and D.-H. Lee, *Phys. Rev. B* **79**, 014505 (2009).
- <sup>31</sup>I. A. Nekrasov, Z. V. Pchelkina, and M. V. Sadovskii, *JETP Lett.* **88**, 144 (2008).
- <sup>32</sup>F. J. Ma, Z. Y. Lu, and T. Xiang, arXiv:0806.3526 (unpublished).
- <sup>33</sup>D. J. Singh, *Phys. Rev. B* **78**, 094511 (2008).